# Synergistic roles of the proteasome and autophagy for mitochondrial maintenance and chronological lifespan in fission yeast

Kojiro Takeda[a], Tomoko Yoshida[b], Sakura Kikuchi[a], Koji Nagao[a], Aya Kokubu[a], Tomáš Pluskal[a], Alejandro Villar-Briones[a], Takahiro Nakamura[c], and Mitsuhiro Yanagida[a,c,1]

[a]G0 Cell Unit and [b]Electron Microscope Room, Okinawa Institute of Science and Technology (OIST), Uruma, Okinawa 904-2234, Japan; and [c]Core Research for Evolutional Science and Technology Research Program, Japan Science and Technology Corporation, Graduate School of Biostudies, Kyoto University, Sakyo-ku, Kyoto 606-8501, Japan

Regulations of proliferation and quiescence in response to nutritional cues are important for medicine and basic biology. The fission yeast *Schizosaccharomyces pombe* serves as a model, owing to the shift of proliferating cells to the metabolically active quiescence (designate G0 phase hereafter) by responding to low nitrogen source. *S. pombe* G0 phase cells keep alive for months without growth and division. Nitrogen replenishment reinstates vegetative proliferation phase (designate VEG). Some 40 genes required for G0 maintenance were identified, but many more remain to be identified. We here show, using mutants, that the proteasome is required for maintaining G0 quiescence. Functional outcomes of proteasome in G0 and VEG phases appear to be distinct. Upon proteasome dysfunction, a number of antioxidant proteins and compounds responsive to ROS (reactive oxygen species) are produced. In addition, autophagy-mediated destruction of mitochondria occurs, which suppresses the loss of viability by eliminating ROS-generating mitochondria. These defensive responses are found in G0 but not in VEG, suggesting that the main function of proteasome in G0 phase homeostasis is to minimize ROS. Proteasome and autophagy are thus collaborative to support the lifespan of *S. pombe* G0 phase.

cell cycle | cellular quiescence | proteolysis | mitochondria

The transition between cell proliferation and G0/quiescent phase is finely controlled in response to extracellular conditions, such as growth factors and nutrient availability (1–3). The regulation of entry and exit to and from G0 phase is strongly relevant to tumorigenesis and tissue regeneration. Failure to maintain terminally differentiated cells in the healthy G0 phase may also lead to diseases such as neurodegeneration. Therefore, regulations of G0 entry, exit, and maintenance are medically important topics.

The fission yeast *Schizosaccharomyces pombe* has been adopted as an excellent model organism for cell cycle research and cell biology, owing to its genetic tractability and similarity to higher eukaryotic cells. Like mammalian cultured cells, which are introduced to G0 phase by serum starvation (1), proliferating cells of the fission yeast enter G0 phase in response to low nitrogen (4–6). Following nitrogen withdrawal from the medium, fission yeast cells immediately cease cell growth, perform division twice, and arrest in G0 phase (G0 entry). Arrested G0 cells are metabolically active, viable for more than 1 month (G0 maintenance), and reinstate proliferation by nitrogen replenishment (G0 exit). We take advantage of this feature of fission yeast and adopt this yeast as a model organism to study the regulatory mechanisms of G0 phase. Previously, we identified seven genes required for G0 entry and 36 genes for maintenance (5, 6), including regulators of transcription, chromatin dynamics, vesicle transport, and the actin cytoskeleton. However, many other factors may remain unidentified.

The ubiquitin/proteasome system, a major proteolytic mechanism in the cell (7), is one possible candidate pathway that may be essential for G0 phase. The ubiquitin/proteasome system is involved in cellular essential pathways, such as cell cycle control and protein quality control. The proteasome is required for M-phase progression (8), because the proteasome is responsible for the degradation of the mitotic regulators cyclin B and securin (9–13). In fission yeast, the proteasome is localized to the nucleus, which guarantees the rapid degradation of Cdc13/cyclin B and Cut2/securin in the nucleus (14–16). In G0 phase, however, the essential roles of the proteasome have not been understood well so far. In this study, we attempt to elucidate essential proteasomal functions specific to G0 phase. We found the proteasome complex is exported from the nucleus to the cytoplasm upon G0 entry. Inactivation of the proteasome in G0 phase is lethal and leads to the accumulation of cellular reactive oxygen species (ROS) and massive degradation of mitochondria by autophagy (mitophagy), which inhibits further accumulation of ROS. We suggest that the proteasome and selective mitophagy cooperatively contribute to G0 maintenance via reducing lethal accumulation of ROS.

## Results

Striking alteration of the 26S proteasome localization was observed during the shift from VEG to G0 phase of *S. pombe*. Green fluorescent protein (GFP) tagged to α4 (20S component) or Pad1/Rpn11 (19S component) was chromosomally integrated under the native promoter and used to locate the 26S proteasome. In VEG, the proteasome is enriched in the nucleus and nuclear envelope (14–16). In G0, nuclear localization signals of α4- and Pad1-GFP were greatly diminished with the increase of cytoplasmic GFP signals, whereas the signal on the nuclear periphery persisted (Fig. 1A and Fig. S1; G0 and VEG cells are, respectively, round and rod shaped). The signals were not intrinsic fluorescence, as cells without GFP tagging showed no fluorescence (Fig. 1A). The proteasome signals remained in the nucleus for 6 h after the removal of nitrogen (–N), when most cells had finished the second division and were competent to mate if cells with the opposite mating type existed. The nuclear proteasome was diminished at 12 h at the timing of G0 entry (6) (Fig. 1B). The level of proteasome subunit was unchanged during VEG to G0 transition, whereas the level of Cdc13 mitotic cyclin was greatly reduced (6) (Fig. 1C). The cytoplasmic α4-GFP signal returned to the nucleus following treatment with the Crm1/exportin inhibitor
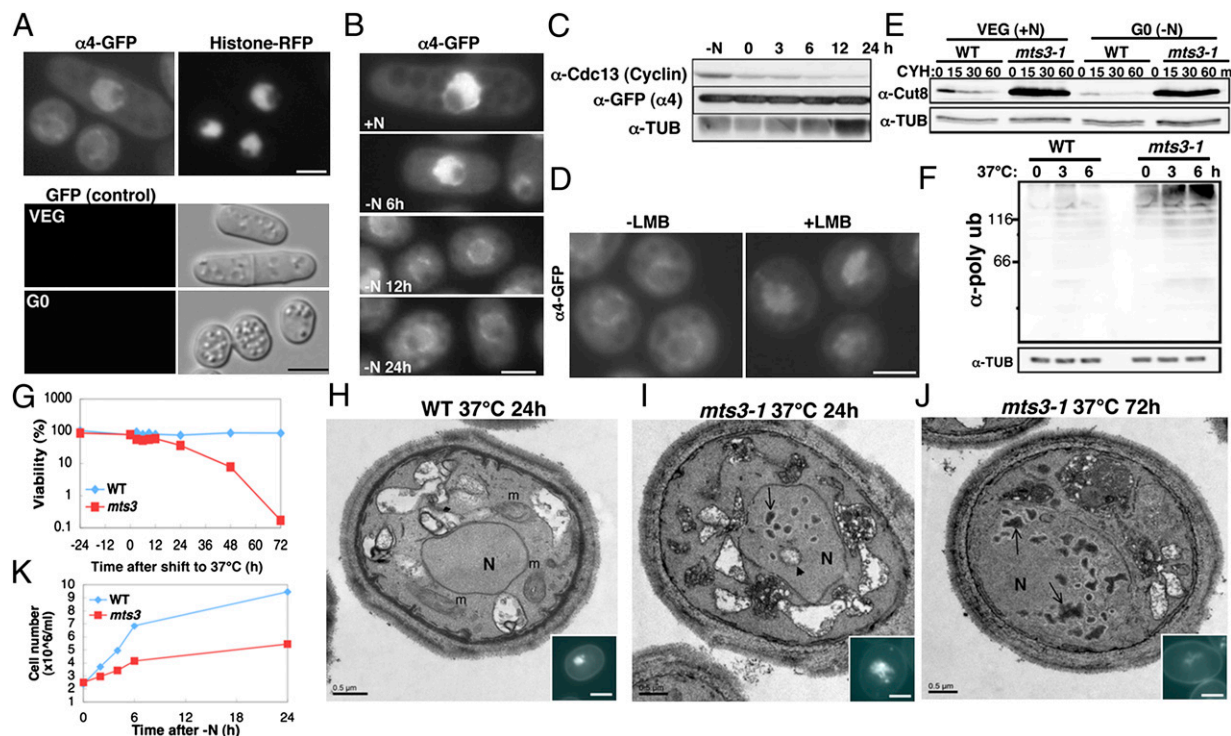
**Fig. 1.** Proteasome-enriched cytoplasm is required for the maintenance of G0 cells. (*A Upper*) Proteasome localization in VEG and G0. α4 subunit and histone H2A were tagged with green and red fluorescent protein, respectively. G0 cells (*A Lower Left*, two round cells) and VEG cells (*A Upper Right*, rod-shaped cell) were independently prepared and mixed on a glass slide. (Scale bar: 2.5 μm.) (*A Lower*) negative controls of no-GFP tagged strain. (Scale bar: 5 μm.) (*B*) Time-course analysis of proteasome localization after –N. (*Vc*) Protein amounts in *B*. α-TUB represents α-tubulin as a loading control. (*D*) Incubating G0 culture with 250 nM leptomycin B for 8 h induced a change in the proteasome localization from the cytoplasm to the nucleus. (*E*) The half-life of Cut8, a proteasome substrate, was examined in both G0 and VEG of WT and *mts3-1*. Proteins were extracted at the indicated time points after adding cycloheximide (100 μg/mL), and proteins were detected by immunoblotting. (*F*) The amount of polyubiquitinated proteins was examined in both WT and *mts3-1* mutants in G0. (*G*) The change of viabilities of WT and *mts3-1* were in G0. (*H–J*) TEM analysis of G0 cells. (Scale bars: 0.5 μm.) Arrow, an electron-dense deposit; arrowhead, the lipid droplet in the nucleus; m, a mitochondrion (no mitochondria were visible in *I* and *J*; N, nucleus. (*Insets*) Fluorescent images of chromosomal DNA stained by DAPI. (Scale bars: 2.5 μm.) (*K*) *mts3-1* mutant cells divided once after –N, whereas WT divided twice.

leptomycin B (LMB) (17) (Fig. 1*D*), indicating that the proteasome export to cytoplasm increased at the G0 shift.

To examine whether proteasome-mediated proteolysis existed in G0 phase, we first isolated the 26S proteasome from both VEG and G0 extracts and analyzed the compositions by mass spectrometry (Fig. S2). Reported subunits and accessory proteins of the 26S complex (18) were all present in both VEG and G0, indicating that the regular 26S proteasome existed in G0. Next, proteolysis and ubiquitination in G0 were examined using *mts3-1* (8), a temperature-sensitive mutant of the proteasome subunit Mts3/Rpn12. Cut8 (a proteasomal localization factor whose degradation in VEG depends on proteasomal activity) (15, 16) found to be short-lived in G0 like in VEG phase (Fig. 1*E*). After the addition of cycloheximide, a protein synthesis inhibitor, the level of Cut8 was diminished within 15 min in both VEG and G0 phase in wild type (WT), but not in the *mts3-1*, suggesting that Cut8 was actively degraded in a proteasome-dependent manner at a similar rate in both VEG and G0. Indeed, the level of polyubiquitinated proteins in G0 was already high in *mts3-1* at a permissive temperature (26 °C), and further increased at the restrictive temperature (37 °C; Fig. 1*F*). These findings established that 26S proteasome-mediated proteolysis was active in G0 phase.

The proteasome was essential for maintenance of the viability in G0. The *mts3-1* mutant decreased to 40% viability after 24 h at 37 °C, which further decreased to 0.1% after 72 h at 37 °C in G0 (Fig. 1*G*). WT sustained high viability (>80%) after 72 h at 37 °C, and the G0-arrested *mts3-1* cells did not lose viability at all for at least 1 week at 26 °C (Fig. S1). The other proteasome mutant *pad1-932* also lost the viability in G0 at 37 °C (Fig. S1).

Thin-section transmission electron microscopy (TEM) of WT and *mts3-1* (Fig. 1 *H–J*) revealed abnormalities in cytoplasm and the nucleus in *mts3-1* at 37 °C. First, mitochondria (indicated by m in WT at 37 °C after 24 h; Fig. 1*H*) were greatly diminished in *mts3-1*. Second, aberrant electron-dense materials (small arrow) and vesicle-like structures (arrowhead) formed in the mutant nucleus after 24 h (Fig. 1*I*) and the nuclear damages further progressed after 72 h (Fig. 1*J*). Nuclear chromatin structure stained by DAPI (Fig. 1*J Inset*) also became deformed. Unexpectedly, the intranuclear vesicle-like structures may be lipid containing, as they were stained by Nile red that was used to reveal lipid droplets (storage particles) normally present in cytoplasm (19) (Fig. S3). A notable mutant phenotype at 26 °C was that *mts3-1* divided only once and arrested after nitrogen withdrawal (Fig. 1*K*), whereas WT cells divided twice before arrest (6). The reason why the second division was omitted in *mts3-1* is unknown.

The decrease of mitochondria in G0 proteasome mutant cells 24 h after the shift to 37 °C was verified by MitoTracker Green stain (20) (Fig. S4). We then made GFP-tagged Sdh2 (succinate dehydrogenase subunit, a mitochondrial protein) integrated at the C terminus of the chromosomal *sdh2*+ gene. Resulting Sdh2-GFP signals expressed under the native promoter in WT and *mts3-1* mutant at 26 °C behave like a mitochondria marker, whereas the GFP signal was greatly diminished in *mts3-1* after 24 h at 37 °C (Fig. 2*A* and Fig. S4). The protein levels of Sdh2-GFP and Gcv1-FLAG (mitochondrial glycine decarboxylase, SPAC31G5.14) detected by immunoblot showed the time course decrease in *mts3-1* at 37 °C after 12 h (Fig. 2*B*). The decrease of mitochondrial protein Sdh2-GFP was observed in other proteasome mutants

CELL BIOLOGY

www.manaraa.com

(*pad1-932*, *pts1-732* mutated in the β5 subunit, *ump1-346*, *-620* mutated in the 20S assembly factor) (21) ([Fig. S4](#)). In VEG phase, however, the Sdh2-GFP signal did not decrease at all after a temperature shift to 37 °C, when the mutant ceased dividing completely, and viability was reduced to 15% (Fig. 2C). Immunoblot (Fig. 2D) showed that Sdh2-GFP did not decrease in VEG even after 24 h at 37 °C (viability decreased to 0%). These findings established that the marked degradation of mitochondria occurred specifically in G0 upon proteasomal inactivation.

To determine whether all principal mitochondrial proteins disappeared in *mts3-1* mutant in G0, comprehensive proteomic analyses were performed using liquid chromatography-tandem mass spectrometry (22) (LC-MS/MS; Thermo Fisher LTQ). Proteins were extracted from WT and *mts3-1* cells at 37 °C for 12 h in G0 (control extracts made were from VEG cells cultured for 6 h at 37 °C). To compare abundance of individual proteins, the scatter plots were used (Fig. 2 E–H). Location of each dot (Fig. 2E *Inset*) in the logarithmic *x* and *y* axis indicates the protein abundance (22, 23) in the two extracts: when the levels of proteins between the two samples are identical or similar, the dots are distributed along the central diagonal line. In WT G0 cells, ~2,000 proteins were detected by LC-MS/MS, in which 256 (light blue dots) were mitochondrial proteins (a total of 696 mitochondria proteins among the 5,000 whole proteins reported in the Sanger Institute GeneDB). In two independently cultured WT G0 cell

extracts (37 °C, 12 h; Fig. 2E), 97% of the 1,917 detected proteins were located within the boundary of a 4-fold change in the two samples (indicated by two lines 4.0× and 0.25×). In contrast, 89% of 2,043 proteins detected from WT and *mts3-1* G0 cells (37 °C, 12 h) were within a 4-fold change (Fig. 2F). The abundance of 125 proteins decreased to less than 0.25-fold in *mts3-1* (outside of upper diagonal line), and 60 of them (48%) were mitochondrial proteins (listed in the green columns of [Table S1](#)). The three most greatly reduced (down to 1–5% in comparison with the levels in WT G0) proteins, Sdh2, Cyc1 (cytochrome *c*), and Ilv5 (acetohydroxyacid reductoisomerase), were mitochondrial proteins. These findings showed that many, but not all, mitochondrial proteins reduced their levels in *mts3-1* G0 phase at 37 °C. No particular type of mitochondrial protein was specifically degraded. The experiment was replicated in VEG phase (Fig. 2 G and H). As expected from cytological results, the proteomic decrease of mitochondrial proteins was insignificant.

The scatter plot of G0 proteomics data (Fig. 3A) revealed 110 proteins that showed a >4-fold increase in *mts3-1* versus WT at 37 °C ([Table S2](#)). Among them, the greatest increase (146-fold) was Hsp16, which belongs to the HSP20/alpha-crystallin heat-shock protein family. Hsp16 increased not only by the temperature upshift, but also by cadmium, nutrient starvation, and DNA damage (24). Three others, SPAC11D3.01c (indicated by 1; similar to *N. crasssa* conidation protein 6) and short-chain
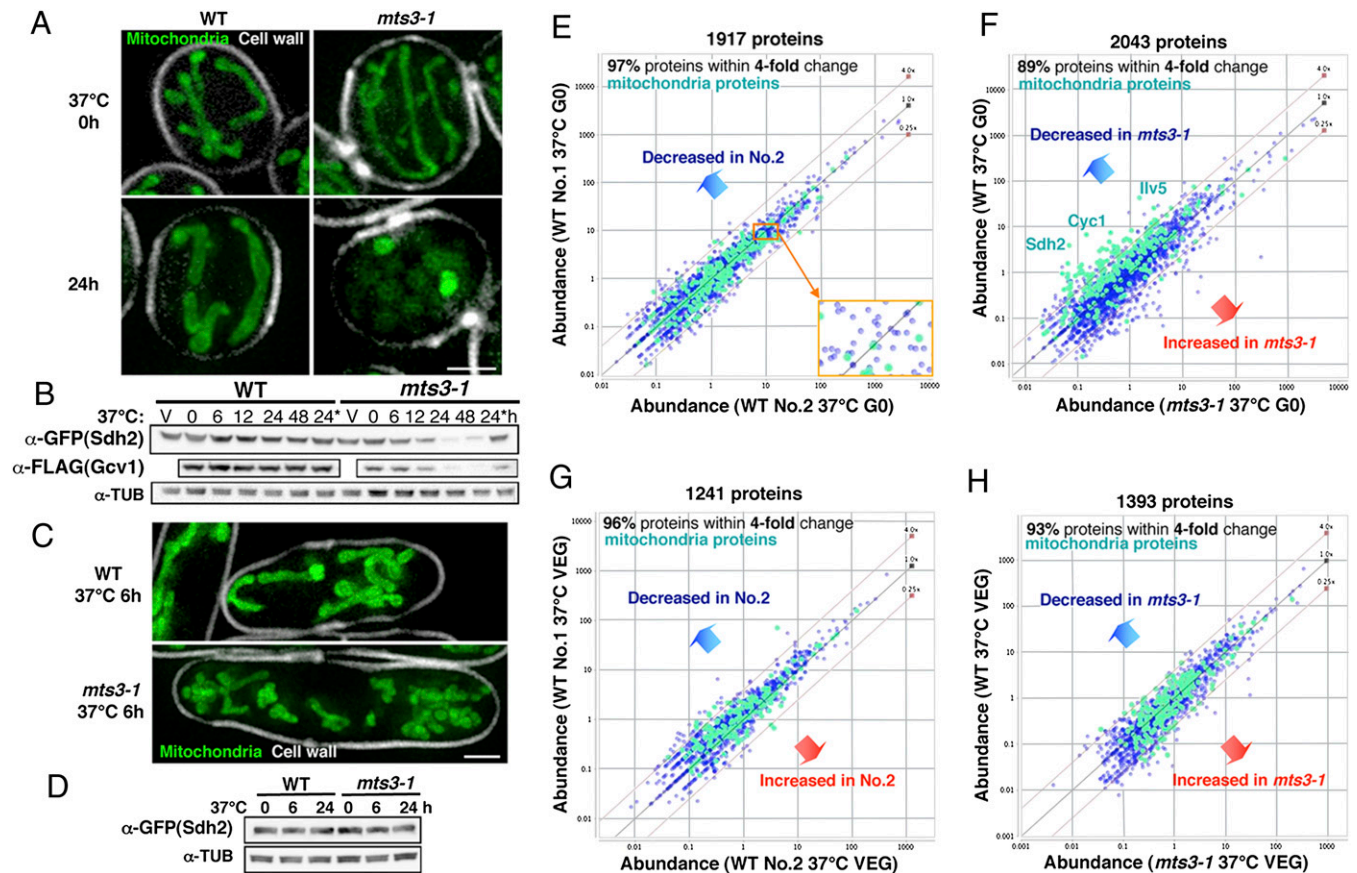


**Fig. 2.** The number of mitochondria was drastically decreased in proteasome mutants in G0. (*A*) Mitochondria were visualized in G0 using Sdh2-GFP as a marker (green). Cell walls were stained by calcofluor (white). (Scale bar: 2 μm.) (*B*) Mitochondrial protein amounts were decreased in *mts3-1* at restrictive temperature (37 °C) in G0. 24* is the sample extracted from the culture at 26 °C for 24 h. (*C*) Mitochondria in VEG. (D) Sdh2-GFP levels remained constant at 37 °C in VEG. (*E*) Scatter plot of emPAI values (protein abundance; see *Methods*) of proteins detected in two different extracts from WT cells, which were independently cultured at 37 °C for 12 h in G0. A part of the plot is enlarged in the inset to reveal each protein. Mitochondrial proteins are shown in green and others in blue. (*F*) Scatter plot of protein abundance in both WT and *mts3-1* cells, which were cultured at 37 °C for 12 h in G0. For both strains, the experiments were repeated twice and the mean emPAI values were analyzed. The names of the proteins with the lowest levels in *mts3-1* are shown. (*G* and *H*) The same experiment as shown in *E* and *F* was performed in VEG.

Takeda et al.

www.manaraa.com

dehydrogenases SPCC663.06c and SPCC663.08c, that prominently (>20-fold) increased in *mts3-1* are known to increase in the presence of $H_2O_2$ (25). SPAC83.17 (4), Multi protein bridging factor 1 (Mbf1) involved in transcriptional regulation of many processes, such as lipid metabolism (26), increased 33-fold in *mts3-1* and is responsive to both heat (>5-fold) and cadmium (~2.5-fold), like Hsp16. Indeed, many (30%) of the 110 proteins that increased >4-fold in *mts3-1* are responsive to $H_2O_2$ and/or cadmium stress (colored dots; see captions of Fig. 3*A*). Proteasome dysfunction seems to activate a number of defensive functions directly ($H_2O_2$ responsive) and indirectly (cadmium responsive) against oxidative stresses (27).

To examine whether metabolic compounds against oxidative stress were produced in G0 *mts3-1*, metabolomic analysis was undertaken using LC/MS (28). Glutathione (GSH) and ergothioneine, both authentic antioxidant metabolites (29), were accumulated in G0 *mts3-1* (>10-fold; Fig. 3*B*). Three duplicate experiments produced a similar increase. GSH and ergothioneine also accumulated in a different proteasome mutant, *pts1* -727 (Fig. S5).

$H_2DCFDA$, a chemical compound that produces fluorescence upon reaction with ROS, was used to stain WT and *mts3-1* cells (30). As seen in Fig. 3*C*, the fluorescent signals were strong in *mts3-1* G0 phase after 24 h (viability = 36%), whereas WT G0 phase cells showed only weak fluorescence. $H_2DCFDA$ signals began to accumulate in *mts3-1* 12 h after the temperature upshift (Fig. S6). At that time point, viability was high (~80%), so that fluorescence was not generated by dead cells. In VEG, there appeared to be no accumulation of ROS in *mts3-1* after the temperature upshift (viability = 15%). The double-staining *mts3-1* G0 cells with $H_2DCFDA$ and MitoTracker showed that the strong signals of $H_2DCFDA$ were located in the mitochondria and nucleus (Fig. 3*D*), suggesting that ROS accumulated in the nucleus and mitochondria in *mts3-1* G0.

To explain the above findings, we speculated that ROS was generated in G0 *mts3-1* due to the breakdown of mitochondria, but the following results suggested that this was not the case.

First, it was found that phenylmethylsulfonyl fluoride (PMSF), a serine protease inhibitor, when added to the culture, inhibited a decrease of Sdh2-GFP and Cox2 in G0 *mts3-1* (Fig. 4*A*). PMSF was reported to inhibit proteolysis in *S. pombe* vacuoles (31), so we examined the involvement of autophagy pathway. The double mutant of *mts3-1* and deletion Δ*atg8* was constructed (Atg8, an LC3 homolog, is involved in autophagosome formation) (32) and observed using Sdh2-GFP as the marker of mitochondrial destruction. In the double-mutant cells at 24 h (37 °C), the level of Sdh2-GFP did not decrease (Fig. 4*B*) and the mitochondrial degradation was virtually absent (Fig. 4*C*). These findings indicated that mitochondrial degradation in *mts3-1* required Atg8. A surprising outcome was the synthetic lethality of the double mutant in G0 as shown in Fig. 4*D*. The viability of the double mutant sharply decreased after 12 h, and reached 3%, whereas more than 50% viability was maintained in the single *mts3-1*. Corroborating finding was that the accumulation of $H_2DCFDA$ fluorescence was observed already in the double mutant at 6 h, whereas there was no accumulation in the single *mts3-1* at 6 h (Fig. 4*E*). After 24 h, fluorescence was much greater in the double-mutant *mts3-1* Δ*atg8* than in *mts3-1*. As shown in Fig. 4*E* and Fig. S7, $H_2DCFDA$ signals were strong along the mitochondria in *mts3-1* Δ*atg8*, suggesting that autophagy actually caused the reduction of ROS (perhaps within mitochondria) by degrading mitochondria that was impaired in G0 phase *mts3-1*. In Δ*atg8* cells, the $H_2DCFDA$ fluorescence was not significantly different from WT after 24 h (Fig. S7). After longer incubation in G0 (2-3 weeks) at 26 °C, however, the fluorescence was stronger in Δ*atg8* cells, accompanied with a viability decrease after 21 days (Fig. S7). Therefore, autophagy is also required for long-term survival in G0, though the degree is much less than proteasome function. This is consistent with the previous report (31).

N-acetyl cysteine (NAC), an antioxidant, was added to the G0 culture to examine the effect on $H_2DCFDA$ fluorescence (Fig. 4*E*). Fluorescence in *mts3-1*Δ*atg8* was significantly reduced after 6 h and 24 h. Consistently, the viability of the double mutant with
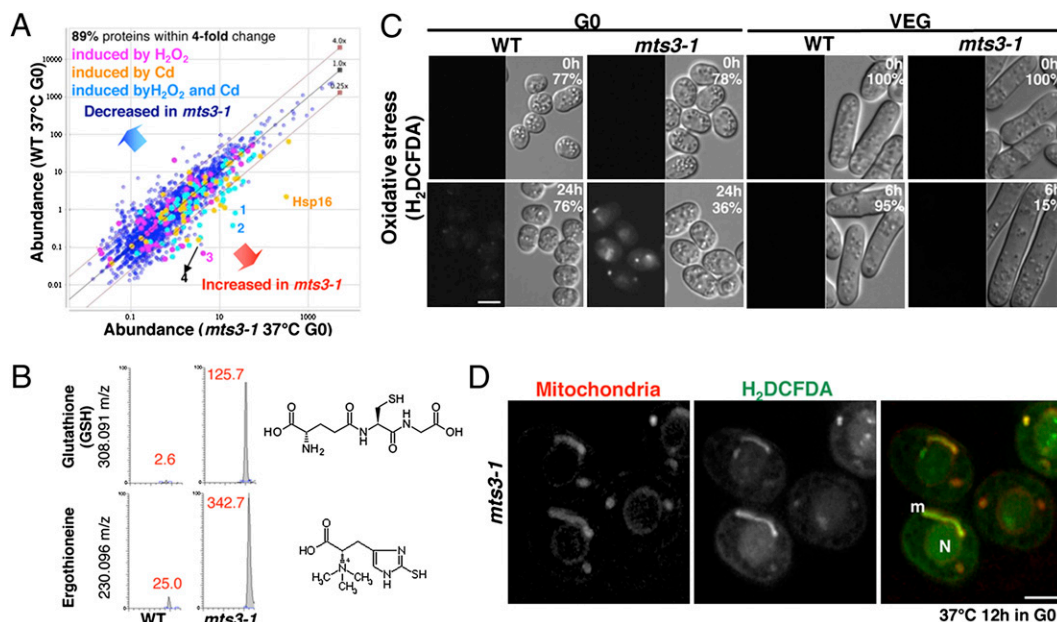


**Fig. 3.** ROS accumulated in proteasome mutants in G0. (*A*) The same experiment as shown in Fig. 2*F*. Purple, yellow, and pale blue dots represent proteins, which are transcriptionally induced over 3-fold by $H_2O_2$, cadmium (Cd), and both of them, respectively. The proteins with the highest levels in *mts3-1* are indicated by numbers (1~4; see text). (*B*) Metabolic analysis revealed glutathione (reduced form; GSH) and ergothioneine in *mts3-1* in G0. Chromatogram patterns of each compound separated by HPLC. Values in red represent the integrated peak area (*y* axis). See text and *Methods*. (*C*) The $H_2DCFDA$ signal, an indicator of ROS, accumulated in *mts3-1* cells in G0, but not VEG. The time points shown are 0 h and 24 h after the temperature shift to 37 °C. The viability at each time point is also presented (%). (Scale bar: 5 μm.) (*D*) The $H_2DCFDA$ (green) signal accumulated in the nucleus (N) and mitochondria (m) in *mts3-1* cells 12 h after the temperature shift. Mitochondria were stained by MitoTracker Orange (red; Invitrogen). (Scale bar: 2 μm.)
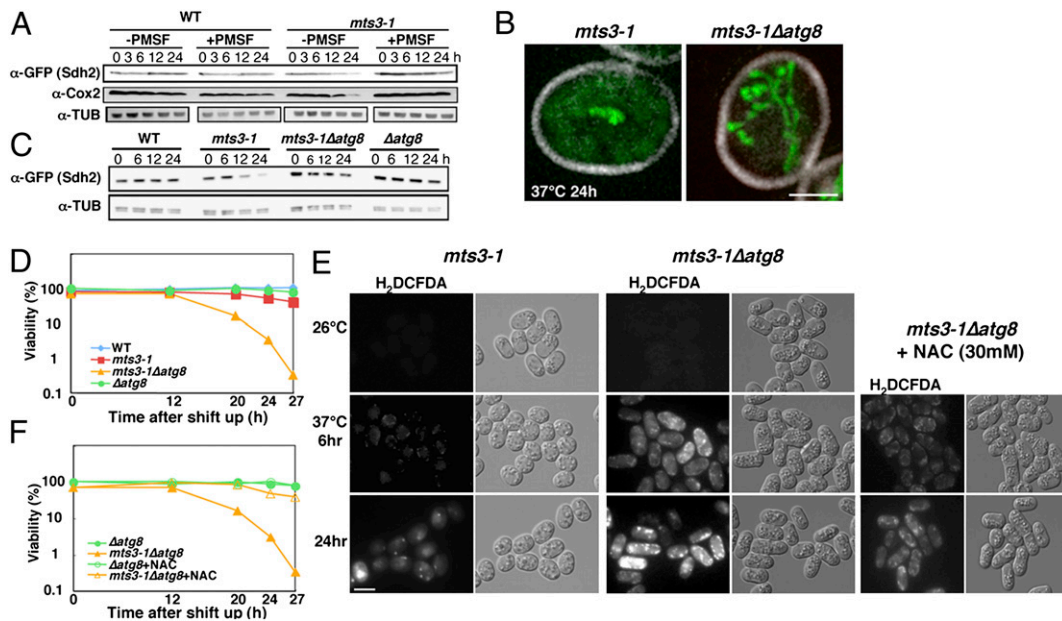
**CELL BIOLOGY**

**Fig. 4.** Autophagy is involved in degrading mitochondria to reduce the lethal accumulation of oxidative stress in G0. (*A*) PMSF (2 mM) inhibited the decrease of mitochondrial proteins in *mts3-1* in G0. (*B*) Sdh2-GFP signals (green) maintained a tubular structure in the *mts3-1Δatg8* double mutant, whereas the signal was greatly decreased in the *mts3-1* mutant. Both cells were cultured in G0 at 37 °C for 24 h. (Scale bar: 2 μm.) (*C*) The amount of Sdh2-GFP proteins was kept constant in the *mts3-1Δatg8* double mutant. (*D*) The viabilities of WT (blue), *mts3-1* (red), *mts3-1Δatg8* (orange), and *Δatg8* (green) were examined after the temperature shift to 37 °C in G0. (*E*) The accumulation of oxidative stress was examined using H₂DCFDA. In the *mts3-1Δatg8* double mutant, but not in *mts3-1*, stronger H₂DCFDA signals appeared 6 h after the temperature shift. At 24 h, the signal in the double mutant was still stronger than that in *mts3-1*. The addition of 30 mM N-acetyl cysteine (NAC) reduced H₂DCFDA signal intensity in the double mutant at 6 and 24 h. (Scale bar: 4 μm.) (*F*) NAC treatment rescued the viability of the *mts3-1Δatg8* double mutant. Orange solid triangle, culture without NAC; orange empty triangle, culture with NAC.

NAC was much higher (83%, 47%, and 39%, respectively, at 20, 24, and 27 h) than the viability of double mutant without NAC (16%, 3%, and 0.3%, respectively; Fig. 4*F*). The severe lethality of the double mutant might thus be due to the abundance of ROS. Taken together, we concluded that mitochondrial degradation by autophagy is one of many anti-ROS protection events that occurred after proteasome dysfunction in G0 phase.

## Discussion

A principal conclusion in this study is that *S. pombe* G0 cells require proteasome function during the maintenance of G0 quiescence. This conclusion was obtained using several ts mutants in the 26S proteasome subunits. Proteasome genes belong to the group of super housekeeping (6) genes because of their necessity for both proliferation and quiescence. Note that only 25% of the essential genes in VEG are also needed for G0 maintenance (6); many genes essential for proliferation, such as cell division and DNA replication, are not necessary for G0 maintenance. The second conclusion is that proteasome functions are quite different between G0 and VEG phase. This is based on striking defective phenotypes of proteasome mutants in G0 phase, regarding the huge increase of oxygen stress-responsive compounds and the massive decrease of mitochondria that did not occur in VEG phase. How this difference is explained? The targets of proteasome may change from VEG to G0 (more cytoplasmic ones in G0), which may lead to the export of proteasome to cytoplasm in G0 cells. In carbon-starved cells of the fission yeast, the proteasome is also exported reversibly to the cytoplasm (33). Necessity of recycling proteins in G0 (6) may require a number of cytoplasmic activities for proteasome, whereas in VEG events, such as replication, rRNA transcription, mitosis, and chromatin dynamics occur in the nucleus. Actual targets of proteasome in G0 remain to be clarified, however. In the quiescent/stationary phase of *Saccharomyces cerevisiae*, Aah1p (adenine deaminase) was reported

as a substrate of the proteasome, whereas its proteolysis is not required for the maintenance of the quiescence (34).

The third, closely related to the second, conclusion of this study is that proteasome dysfunction in G0 elicits defensive responses, mainly the production of antioxidant components and the degradation of mitochondria by autophagy. These defensive responses were not found in VEG cells, suggesting that proteasome functions in G0 are directly or indirectly involved in minimizing ROS. We provide evidence that viability loss in G0 is caused by the accumulation of oxidative stress. In addition, autophagy-mediated mitochondrial degradation in fact saved proteasome mutant G0 cells. In other words, proteasome collaborates with autophagy in supporting the longevity of G0 cells. Beside the loss of viability, physically aberrant structures were observed in G0 *mts3-1* mutant. Initially observed were the accumulation of electron-dense materials and the internal vesicles in the nucleus. At this timing, viability was high, suggesting that an abnormality in nuclear envelope or nuclear-cytoplasmic shuttling might be initial events that lead to the accumulation of ROS and mitochondrial dysfunction. Note that most of mitochondrial proteins are encoded by chromosomal genes. Aberrant mitochondria possibly producing a bulk of ROS then form, which in turn activate autophagy-dependent mitochondrial degradation. Our findings are consistent with this hypothesis. Proteasome and autophagy seem to support life of nondividing G0 phase cells (chronological lifespan). Our metabolomic and proteomic analyses identify antioxidant metabolites (glutathione, ergothioneine) and many ROS-defensive proteins that increase their levels in *mts3-1* G0 cells. In mammalian neurons, inactivation of the proteasome leads to ROS accumulation, mitochondrial injury, and cell death (35–37), which are related to neurodegeneration. Injured mitochondria may be degraded by autophagy (mitophagy). Recent studies suggested that several proteins are involved in mitophagy, such as Atg32 (in budding yeast) (38, 39) and Park2 (E3 ligase responsible for Parkinson disease) (40, 41). Although neither protein has obvious

Takeda et al.

www.manaraa.com

homologs in *S. pombe*, there could be a common mechanism by which injured mitochondria might be scavenged. Proteasome inhibitors PS-519 and PS-341 are recently developed therapeutics used to treat inflammation and cancer, such as multiple myeloma. The present findings that proteasome dysfunction produces the autophagy-mediated degradation of mitochondria accompanying a number of defensive cellular functions against the elevated level of ROS, which may cause apoptotic removal of the drug-target mammalian cells, might explain some aspects of these drug effects.

## Methods

**Strain, Medium, and Culture.** *S. pombe* heterothallic haploids 972$h^-$ and 975$h^+$ and their derivatives were used. Complete YE and Edinburgh Minimal Media 2 (EMM2) were used to culture *S. pombe* (42). For G0 induction, exponentially growing cells at 26 °C in EMM2 were harvested by vacuum filtration using a nitrocellulose membrane, washed with EMM2-N (EMM2 without nitrogen source), suspended in EMM2-N at a concentration of $2 \times 10^6$ or $5 \times 10^6$ cells/mL, and incubated for 24 h at 26 °C (4). To examine temperature-sensitive mutants, G0 cells of each strain were shifted from 26 °C to 37 °C.

**Immunochemical Methods.** For immunoblot analysis, total proteins were extracted using the trichloroacetic acid (TCA) method. Identical amounts of proteins were separated by SDS/PAGE gel and blotted to nitrocellulose membranes. Anti-Cut8, anti-Pad1, anti-Hxk2, anti-Cox2 (a gift from N. Bonnefoy, Gif-Sur-Yvette, France), anti-α-tubulin (TAT1; a gift from K. Gull, Oxford, UK), anti-GFP (Roche), and anti-FLAG (Sigma) antibodies were used as primary

antibodies. Horseradish peroxidase-conjugated secondary antibodies and an ECL chemiluminescence system (Amersham) were used to amplify signal expression.

**Proteomics and Metabolite Analysis.** To identify immunoprecipitated proteins, we used the procedure reported by Hayashi et al. (22), with some modifications. For whole-proteome analysis, total proteins were extracted, separated by SDS/PAGE, in-gel digested, and analyzed with LC-MS/MS. All MS/MS spectra were searched against an *S. pombe* nonredundant protein database with the Mascot program (Matrix Science). The output data from Mascot was analyzed using in-house software to select reliable peptides and calculate emPAI values (23). For metabolite analysis, we followed methods described previously (28). See *SI Methods* for details.

**Microscopy.** All images were acquired using an AxioPlan 2 (Zeiss) or DeltaVision (Applied Precision) microscope setup. For mitochondrial staining, Mitotracker Green FM and MitoTracker Orange (Invitrogen) were used (20). To obtain mitochondrial images in whole cells, we scanned 21 z-axis sections at a 0.2-μm interval, and the obtained images were deconvolved and projected on a 2D plane. For oxidative stress staining via $H_2DCFDA$ (Invitrogen), we followed the method reported (30). For TEM analysis, see *SI Methods* for details.

1. Zetterberg A, Larsson O (1985) Kinetic analysis of regulatory events in G1 leading to proliferation or quiescence in Swiss 3T3 cells. *Proc Natl Acad Sci USA* 82:5365–5369.
2. Wullschleger S, Loewith R, Hall MN (2006) TOR signaling in growth and metabolism. *Cell* 124:471–484.
3. Gray JV, et al. (2004) "Sleeping beauty": Quiescence in Saccharomyces cerevisiae. *Microbiol Mol Biol Rev* 68:187–206.
4. Su SS, Tanaka Y, Samejima I, Tanaka K, Yanagida M (1996) A nitrogen starvation-induced dormant G0 state in fission yeast: The establishment from uncommitted G1 state and its delay for return to proliferation. *J Cell Sci* 109:1347–1357.
5. Shimanuki M, et al. (2007) Two-step, extensive alterations in the transcriptome from G0 arrest to cell division in Schizosaccharomyces pombe. *Genes Cells* 12:677–692.
6. Sajiki K, et al. (2009) Genetic control of cellular quiescence in S. pombe. *J Cell Sci* 122:1418–1429.
7. Hershko A, Ciechanover A (1998) The ubiquitin system. *Annu Rev Biochem* 67:425–479.
8. Gordon C, McGurk G, Wallace M, Hastie ND (1996) A conditional lethal mutant in the fission yeast 26 S protease subunit mts3+ is defective in metaphase to anaphase transition. *J Biol Chem* 271:5704–5711.
9. Sudakin V, et al. (1995) The cyclosome, a large complex containing cyclin-selective ubiquitin ligase activity, targets cyclins for destruction at the end of mitosis. *Mol Biol Cell* 6:185–197.
10. Yamashita YM, et al. (1996) 20S cyclosome complex formation and proteolytic activity inhibited by the cAMP/PKA pathway. *Nature* 384:276–279.
11. Funabiki H, et al. (1997) Fission yeast Cut2 required for anaphase has two destruction boxes. *EMBO J* 16:5977–5987.
12. Yamano H, Gannon J, Hunt T (1996) The role of proteolysis in cell cycle progression in Schizosaccharomyces pombe. *EMBO J* 15:5268–5279.
13. Zachariae W, Shin TH, Galova M, Obermaier B, Nasmyth K (1996) Identification of subunits of the anaphase-promoting complex of Saccharomyces cerevisiae. *Science* 274:1201–1204.
14. Wilkinson CR, et al. (1998) Localization of the 26S proteasome during mitosis and meiosis in fission yeast. *EMBO J* 17:6465–6476.
15. Tatebe H, Yanagida M (2000) Cut8, essential for anaphase, controls localization of 26S proteasome, facilitating destruction of cyclin and Cut2. *Curr Biol* 10:1329–1338.
16. Takeda K, Yanagida M (2005) Regulation of nuclear proteasome by Rhp6/Ubc2 through ubiquitination and destruction of the sensor and anchor Cut8. *Cell* 122:393–405.
17. Fukuda M, et al. (1997) CRM1 is responsible for intracellular transport mediated by the nuclear export signal. *Nature* 390:308–311.
18. Leggett DS, et al. (2002) Multiple associated proteins regulate proteasome structure and function. *Mol Cell* 10:495–507.
19. Zhang Q, et al. (2003) Schizosaccharomyces pombe cells deficient in triacylglycerols synthesis undergo apoptosis upon entry into the stationary phase. *J Biol Chem* 278:47145–47155.
20. Pozniakovsky AI, et al. (2005) Role of mitochondria in the pheromone- and amiodarone-induced programmed death of yeast. *J Cell Biol* 168:257–269.
21. Ramos PC, Hockendorff J, Johnson ES, Varshavsky A, Dohmen RJ (1998) Ump1p is required for proper maturation of the 20S proteasome and becomes its substrate upon completion of the assembly. *Cell* 92:489–499.
22. Hayashi T, et al. (2007) Rapamycin sensitivity of the Schizosaccharomyces pombe tor2 mutant and organization of two highly phosphorylated TOR complexes by specific and common subunits. *Genes Cells* 12:1357–1370.
23. Ishihama Y, et al. (2005) Exponentially modified protein abundance index (emPAI) for estimation of absolute protein amount in proteomics by the number of sequenced peptides per protein. *Mol Cell Proteomics* 4:1265–1272.
24. Taricani L, Feilotter HE, Weaver C, Young PG (2001) Expression of hsp16 in response to nucleotide depletion is regulated via the spc1 MAPK pathway in Schizosaccharomyces pombe. *Nucleic Acids Res* 29:3030–3040.
25. Chen D, et al. (2003) Global transcriptional responses of fission yeast to environmental stress. *Mol Biol Cell* 14:214–229.
26. Brendel C, Gelman L, Auwerx J (2002) Multiprotein bridging factor-1 (MBF-1) is a cofactor for nuclear receptors that regulate lipid metabolism. *Mol Endocrinol* 16:1367–1377.
27. Monroe RK, Halvorsen SW (2009) Environmental toxicants inhibit neuronal Jak tyrosine kinase by mitochondrial disruption. *Neurotoxicology* 30:589–598.
28. Pluskal T, Nakamura T, Villar-Briones A, Yanagida M (2010) Metabolic profiling of the fission yeast S. pombe: Quantification of compounds under different temperatures and genetic perturbation. *Mol Biosyst* 10.1039/b908784b.
29. Chaudiere J, Ferrari-Iliou R (1999) Intracellular antioxidants: From chemical to biochemical mechanisms. *Food Chem Toxicol* 37:949–962.
30. Marchetti MA, Weinberger M, Murakami Y, Burhans WC, Huberman JA (2006) Production of reactive oxygen species in response to replication stress and inappropriate mitosis in fission yeast. *J Cell Sci* 119:124–131.
31. Kohda TA, et al. (2007) Fission yeast autophagy induced by nitrogen starvation generates a nitrogen source that drives adaptation processes. *Genes Cells* 12:155–170.
32. Kirisako T, et al. (1999) Formation process of autophagosome is traced with Apg8/Aut7p in yeast. *J Cell Biol* 147:435–446.
33. Laporte D, Salin B, Daignan-Fornier B, Sagot I (2008) Reversible cytoplasmic localization of the proteasome in quiescent yeast cells. *J Cell Biol* 181:737–745.
34. Escusa S, Camblong J, Galan JM, Pinson B, Daignan-Fornier B (2006) Proteasome- and SCF-dependent degradation of yeast adenine deaminase upon transition from proliferation to quiescence requires a new F-box protein named Saf1p. *Mol Microbiol* 60:1014–1025.
35. Qiu JH, et al. (2000) Proteasome inhibitors induce cytochrome c-caspase-3-like protease-mediated apoptosis in cultured cortical neurons. *J Neurosci* 20:259–265.
36. Ling YH, Liebes L, Zou Y, Perez-Soler R (2003) Reactive oxygen species generation and mitochondrial dysfunction in the apoptotic response to Bortezomib, a novel proteasome inhibitor, in human H460 non-small cell lung cancer cells. *J Biol Chem* 278:33714–33723.
37. Papa L, Rockwell P (2008) Persistent mitochondrial dysfunction and oxidative stress hinder neuronal cell recovery from reversible proteasome inhibition. *Apoptosis* 13:588–599.
38. Okamoto K, Kondo-Okamoto N, Ohsumi Y (2009) Mitochondria-anchored receptor Atg32 mediates degradation of mitochondria via selective autophagy. *Dev Cell* 17:87–97.
39. Kanki T, Wang K, Cao Y, Baba M, Klionsky DJ (2009) Atg32 is a mitochondrial protein that confers selectivity during mitophagy. *Dev Cell* 17:98–109.
40. Shimura H, et al. (2000) Familial Parkinson disease gene product, parkin, is a ubiquitin-protein ligase. *Nat Genet* 25:302–305.
41. Narendra D, Tanaka A, Suen DF, Youle RJ (2008) Parkin is recruited selectively to impaired mitochondria and promotes their autophagy. *J Cell Biol* 183:795–803.
42. Moreno S, Klar A, Nurse P (1991) Molecular genetic analysis of fission yeast Schizosaccharomyces pombe. *Methods Enzymol* 194:795–823.

CELL BIOLOGY